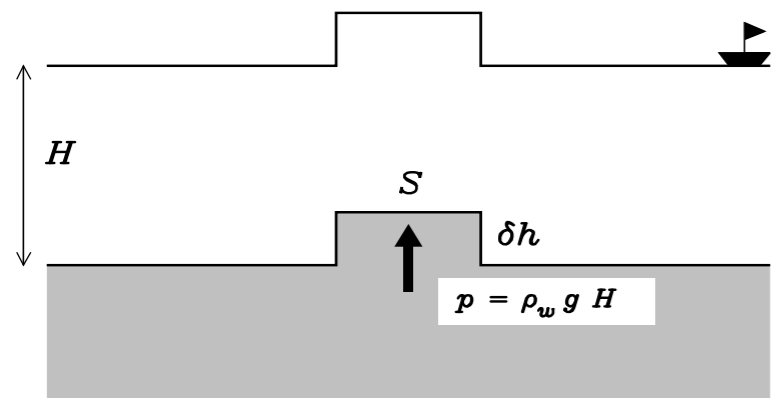
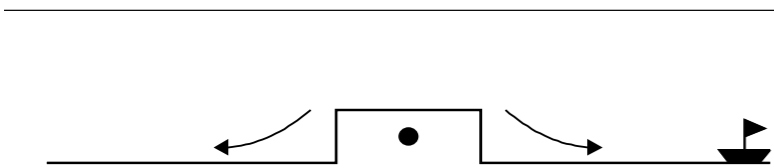


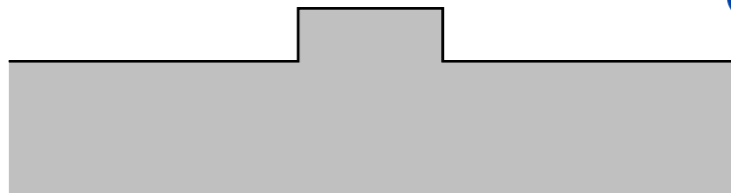
Very basic tsunami physics...



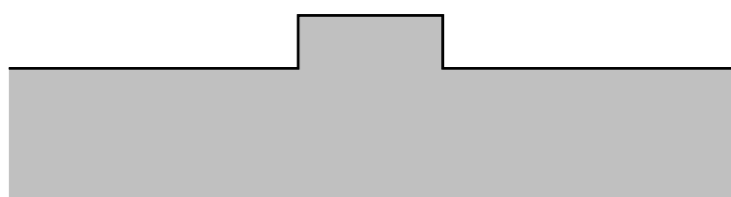
Bottom uplift
&
Waterberg
formation



Center of mass falls...



Potential
energy goes to
tsunami energy



Energy

$$E_R \approx 4.8 + 1.5M$$

$$E_T = \frac{1}{2} \rho g L \lambda (\delta h)^2$$

$$L \sim 10^6 \text{ m}; \lambda \sim 10^4 \text{ m}; \delta h \sim 5 \text{ m}$$

$$E_R \approx 10^{18} \text{ J} \geq 10^2 E_T$$

Wavelength

$$\frac{\lambda}{H} \sim 40; \frac{H}{a} \sim 3 \cdot 10^3$$

$$\lambda \gg H \gg a$$

Tsunami is a shallow-water
gravity wave with great
wavelength and tiny
amplitude

Navier-Stokes equations

Newton's law

+

Conservation of matter

+

Viscosity

$$\rho \frac{\partial \mathbf{v}}{\partial t} + \rho(\mathbf{v} \cdot \text{grad})\mathbf{v} = -\text{grad}(P) - \rho \text{grad}(\phi) + \\ + \eta \Delta \mathbf{v} + (\eta + \eta') \text{grad}(\text{div}(\mathbf{v}))$$

Gravity waves: dispersion

$$F(z) = 2Ae^{-kh} \cosh[k(z+h)]$$

and the boundary at the top gives the dispersion relation for incompressible, irrotational, small amplitude “gravity” waves:

$$\omega^2 = kg[\tanh(kh)]$$

deep water (kh goes to infinity)

$$\omega^2 = kg$$

$$c = \sqrt{\frac{g}{k}} = \sqrt{\frac{g\lambda}{2\pi}}$$

$$u = \frac{\partial \omega}{\partial k} = \frac{1}{2} c = \frac{1}{2} \sqrt{\frac{g}{k}} = \frac{1}{2} \sqrt{\frac{g\lambda}{2\pi}}$$

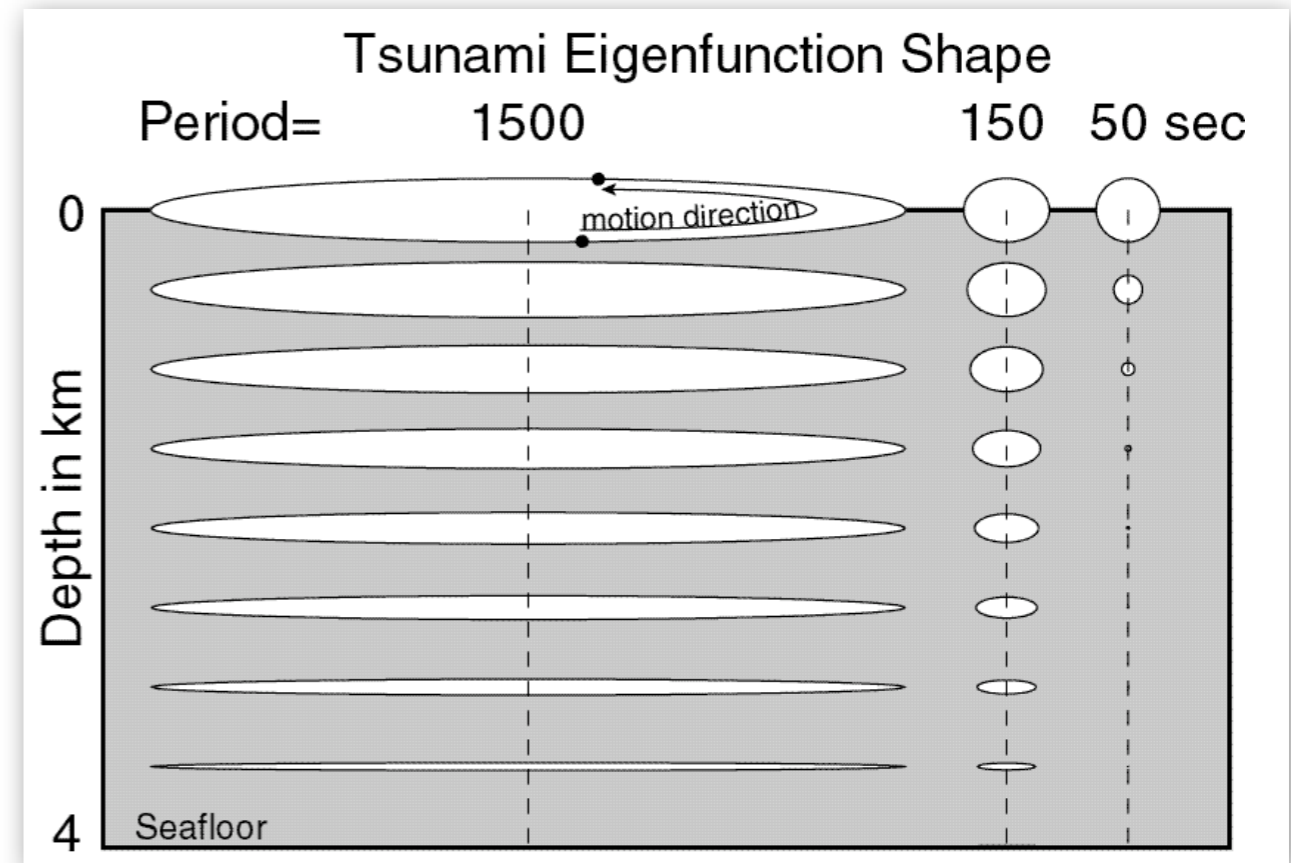
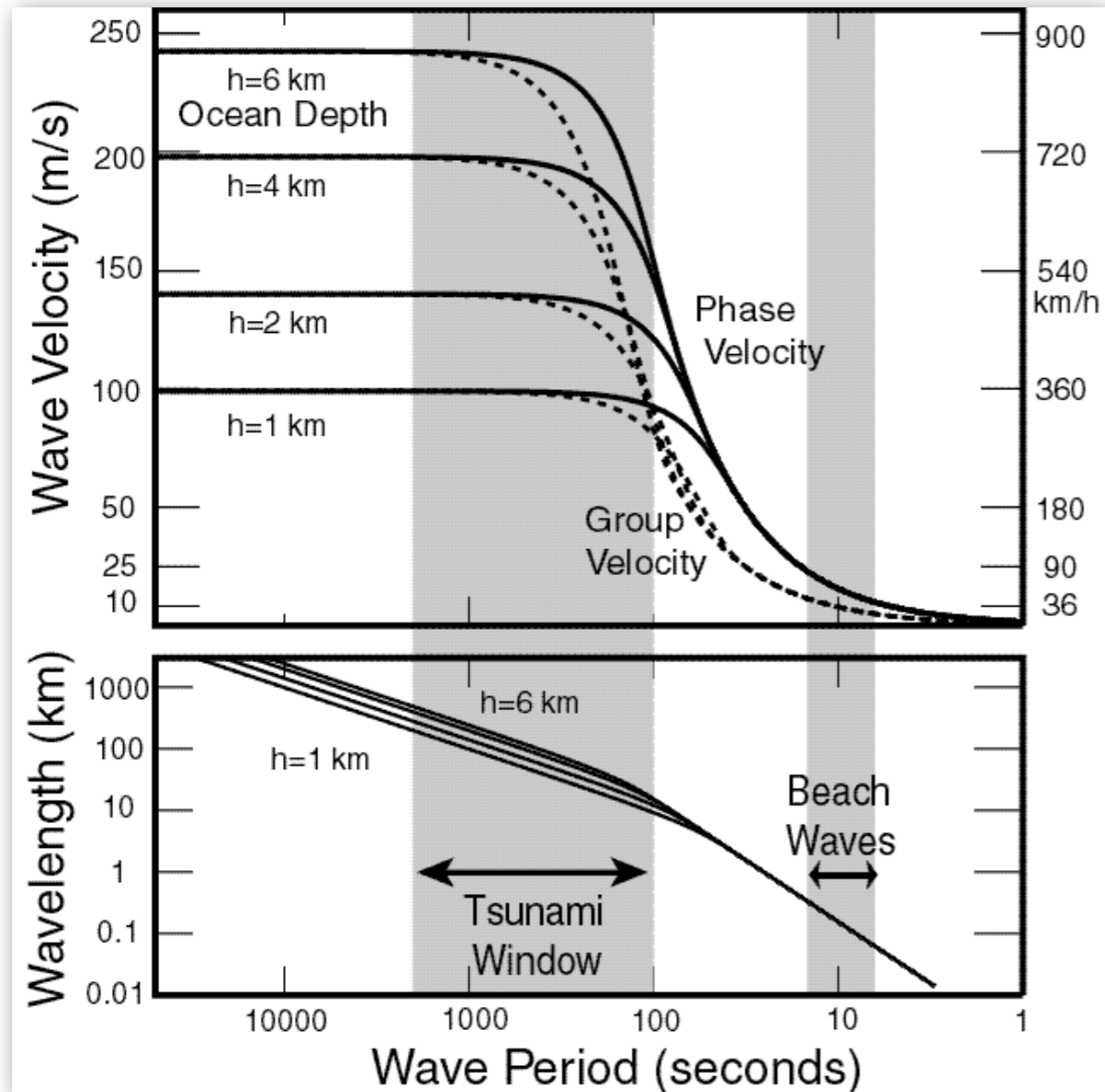
shallow water (kh goes to zero)

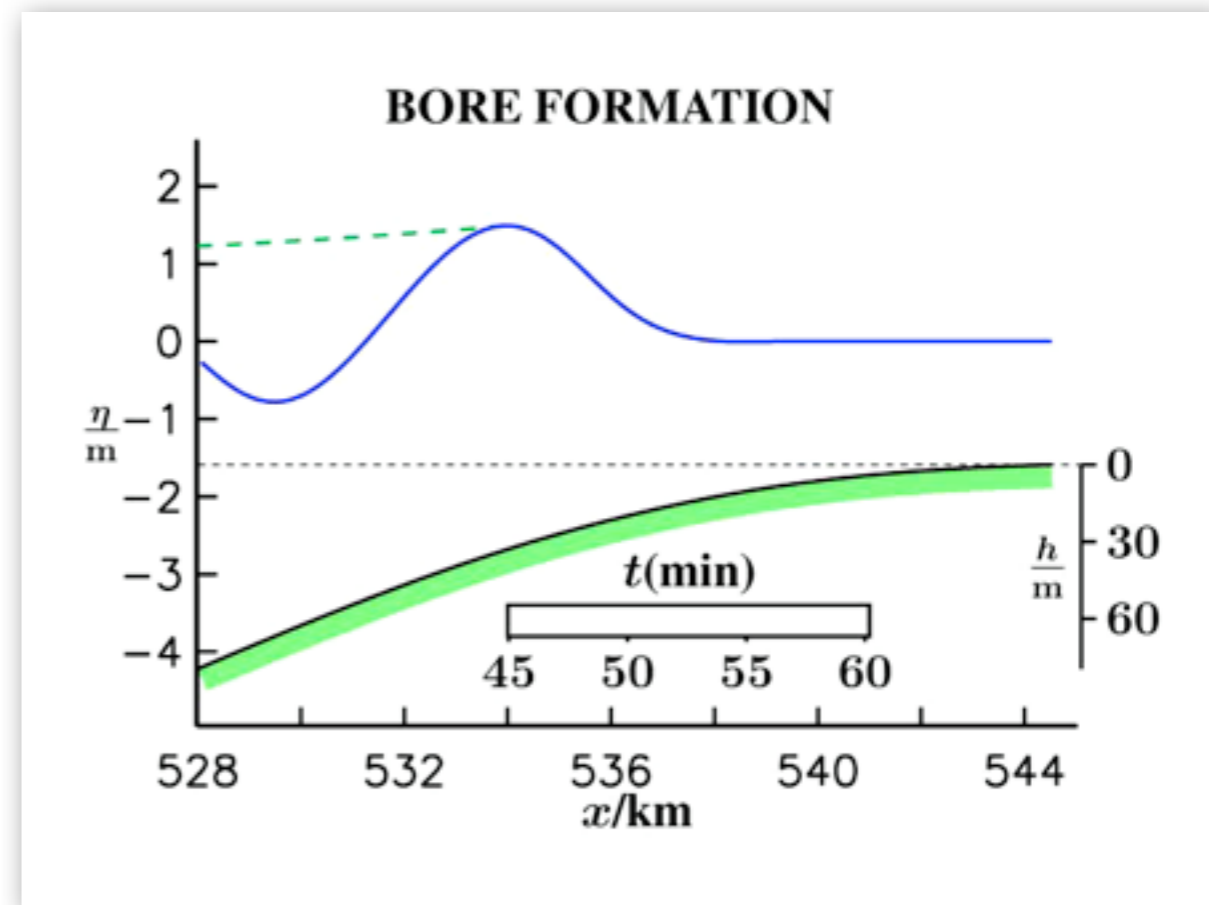
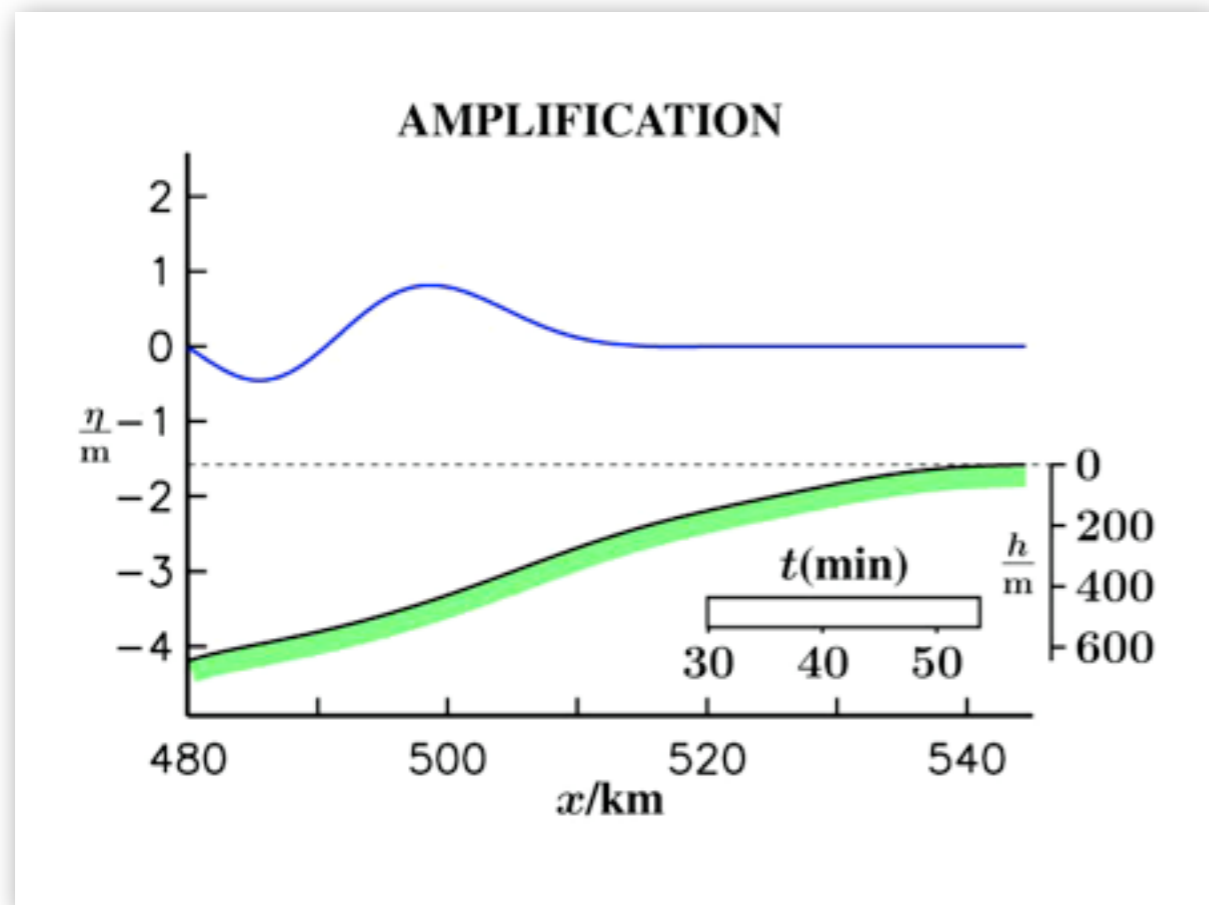
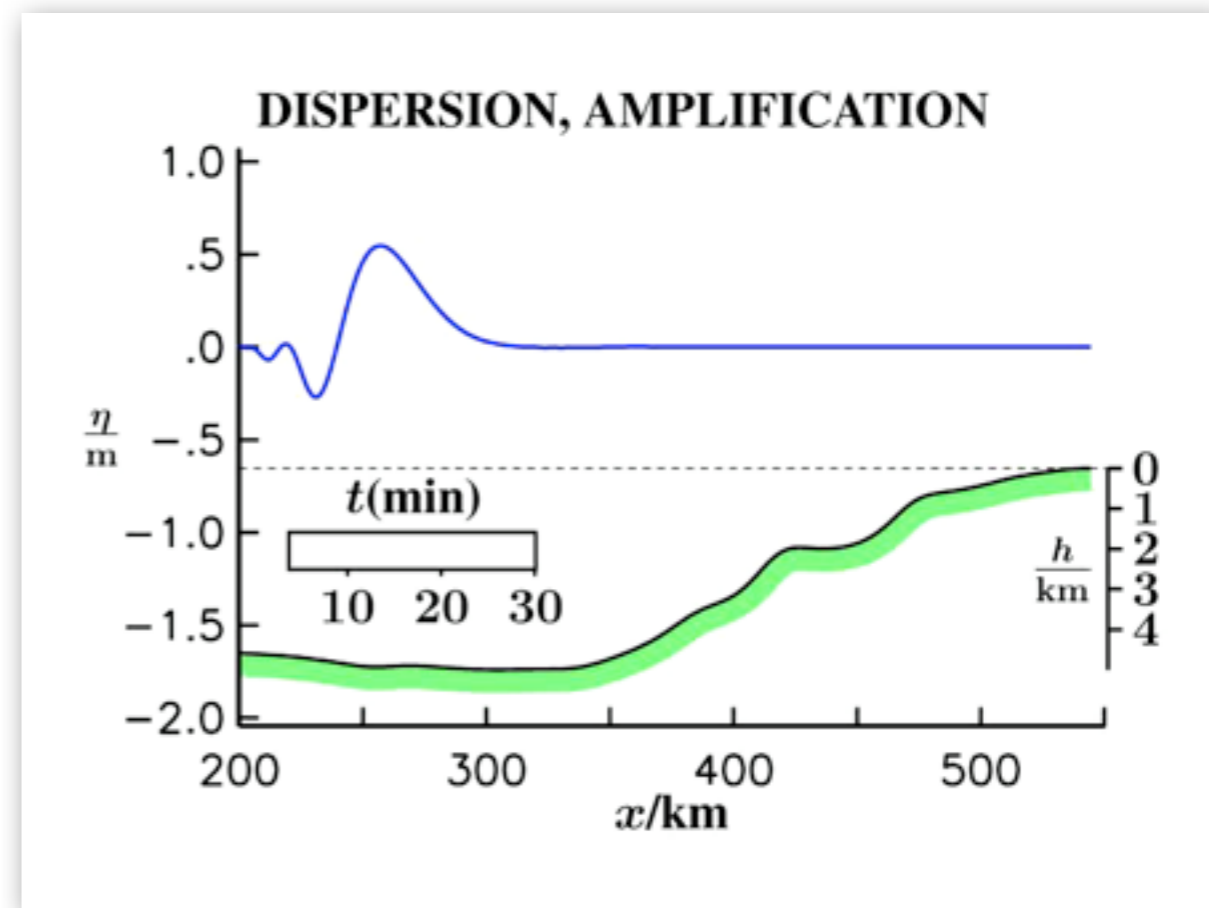
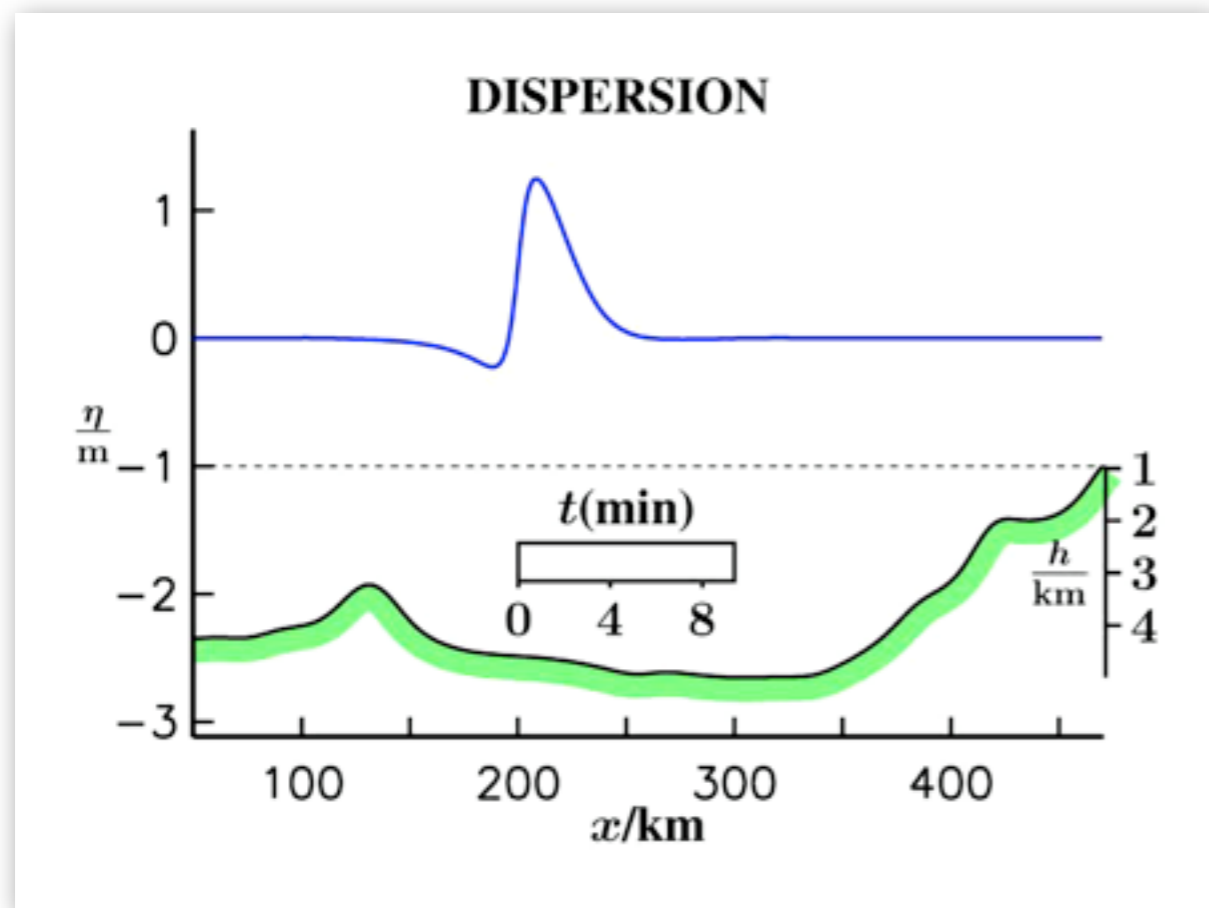
$$\omega^2 = k^2 gh$$

$$c = \sqrt{gh}$$

$$u = \frac{\partial \omega}{\partial k} = c = \sqrt{gh}$$

Tsunami eigenvalues & eigenfunctions





Modal approach - sketch

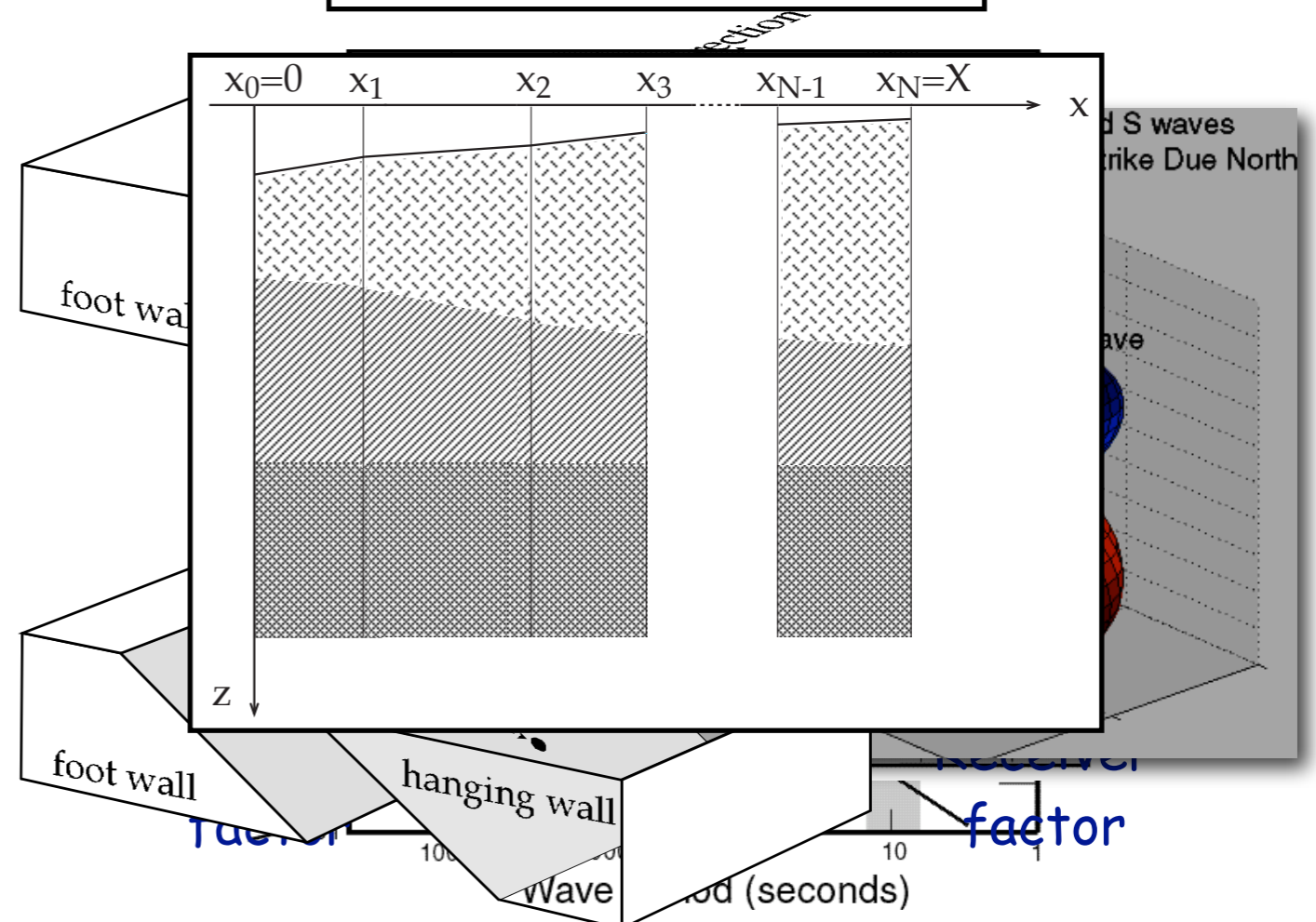
Equations of elastic motion with **gravity** + boundary conditions

FULL coupling between the fluid and solid layers

Eigenvalues & Eigenfunctions

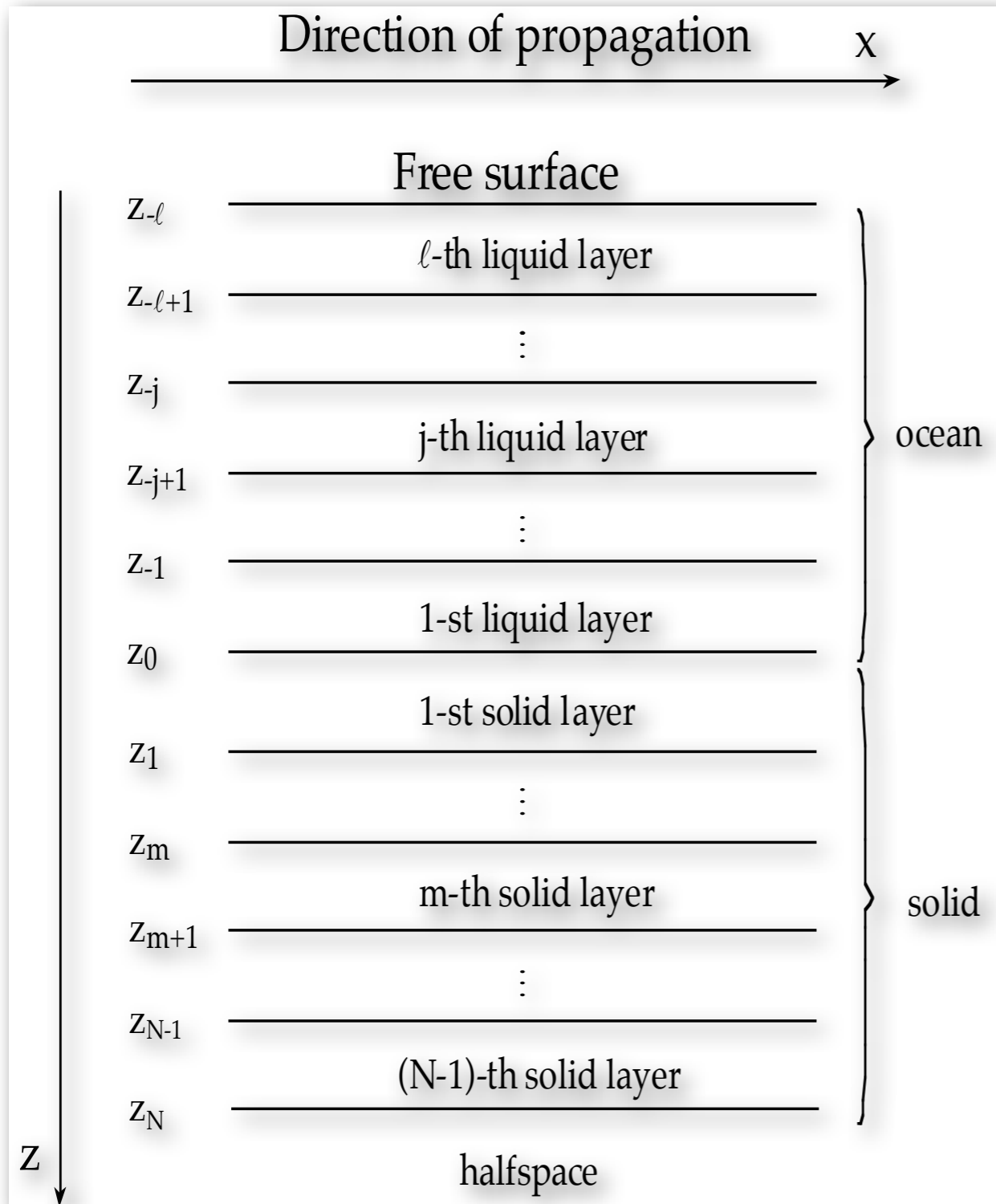
Seismic source excitation

Tsunami mode propagation in LHM



$$U(X, \varphi, z, \omega, t) = \frac{\exp(-i\pi/4)}{\sqrt{8\pi}} \frac{\exp[i\omega(t - \tau)]}{\sqrt{J}} \frac{\chi(h_s, \varphi) R(\omega)}{\sqrt{\omega c} \sqrt{v_g I_1}} \bigg|_s \frac{u(z, \omega)}{\sqrt{v_g I_1}} \bigg|_X$$

Modal approach: formulation



• EQUATIONS OF MOTION

$$\alpha^2 \nabla(\nabla \cdot \mathbf{u}) - g \mathbf{e}_z \nabla \cdot \mathbf{u} = \frac{\partial^2 \mathbf{u}}{\partial t^2}$$

$$\alpha^2 \nabla(\nabla \cdot \mathbf{u}) - \beta^2 \nabla \times (\nabla \times \mathbf{u}) = \frac{\partial^2 \mathbf{u}}{\partial t^2}$$

• BOUNDARY CONDITIONS

$$\alpha^2 \nabla \cdot \mathbf{u} - gw = 0$$

$$w_{-j}(z_{-j}) = w_{-j-1}(z_{-j}) \quad u_{-j}(z_{-j}) = u_{-j-1}(z_{-j})$$

$$p_{-j}(z_{-j} + w_{-j}) = p_{-j-1}(z_{-j} + w_{-j-1})$$

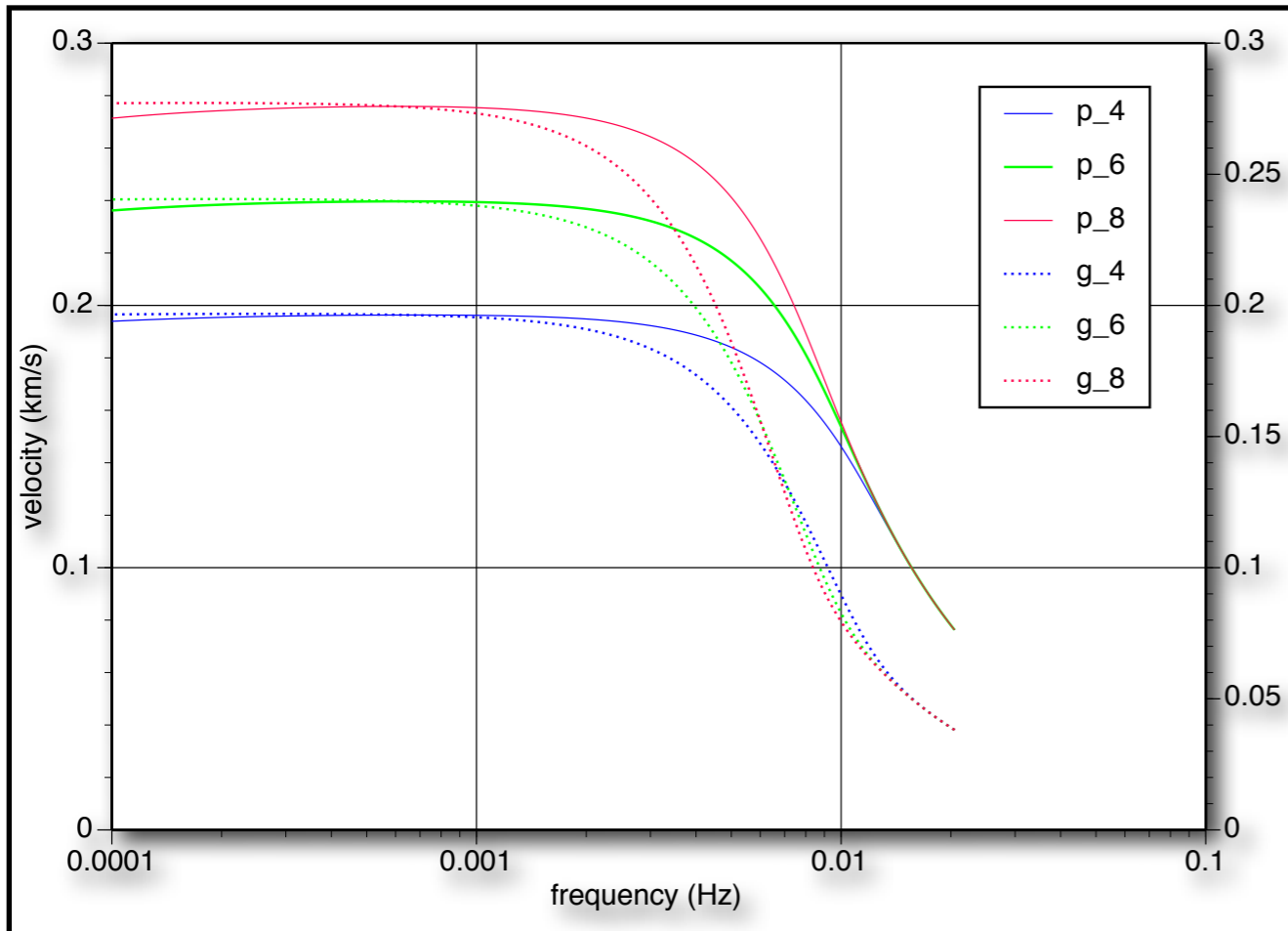
$$w_{-1}(z_0) = w_1(z_0)$$

$$p_{-1}(z_0) = \sigma_1(z_0) \quad 0 = \tau_1(z_0)$$

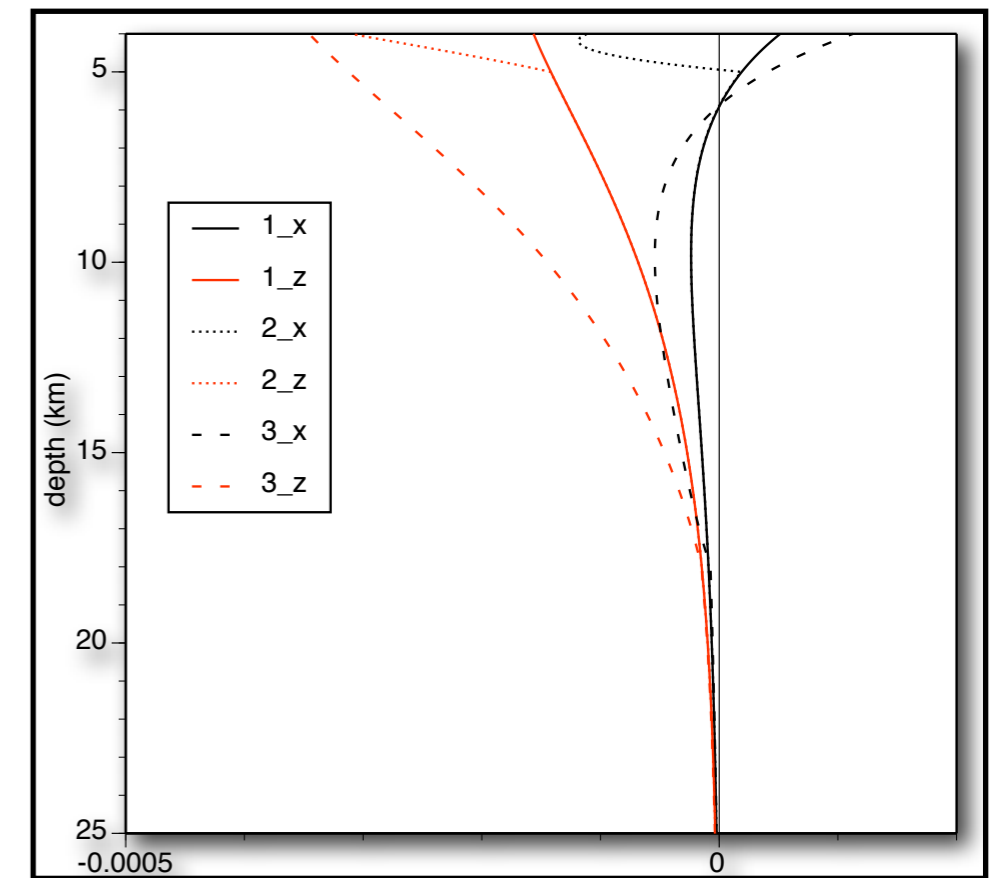
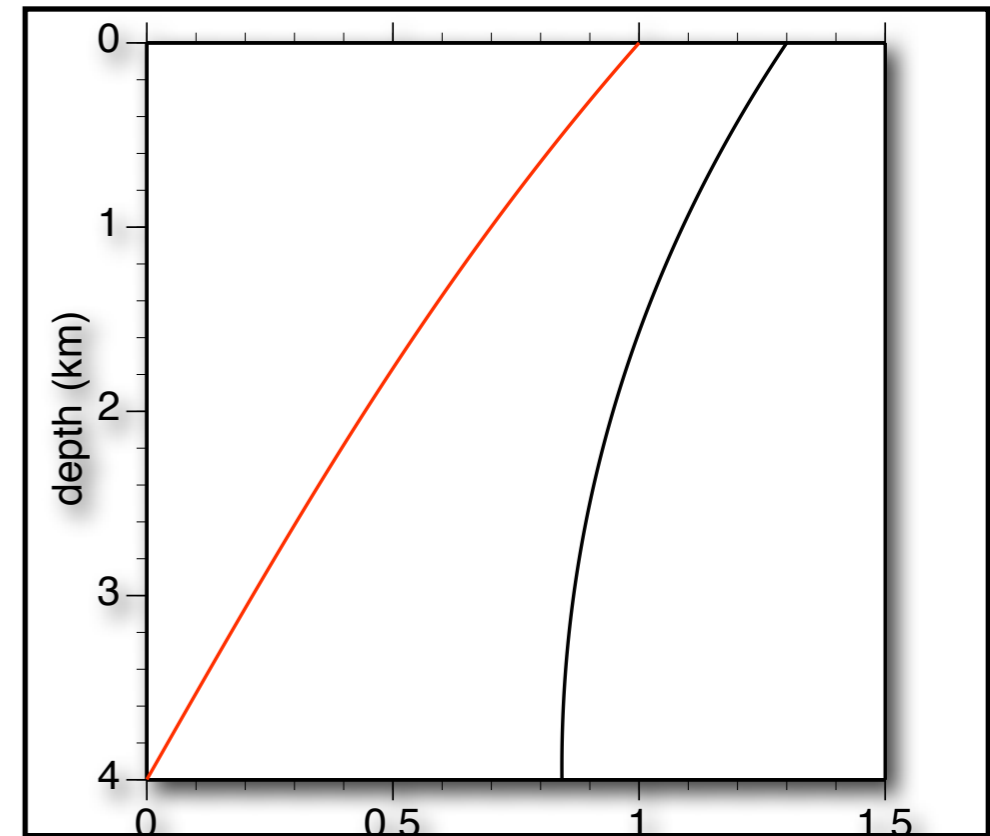
$$w_m(z_m) = w_{m+1}(z_m) \quad u_m(z_m) = u_{m+1}(z_m)$$

$$\sigma_m(z_m) = \sigma_{m+1}(z_m) \quad \tau_m(z_m) = \tau_{m+1}(z_m)$$

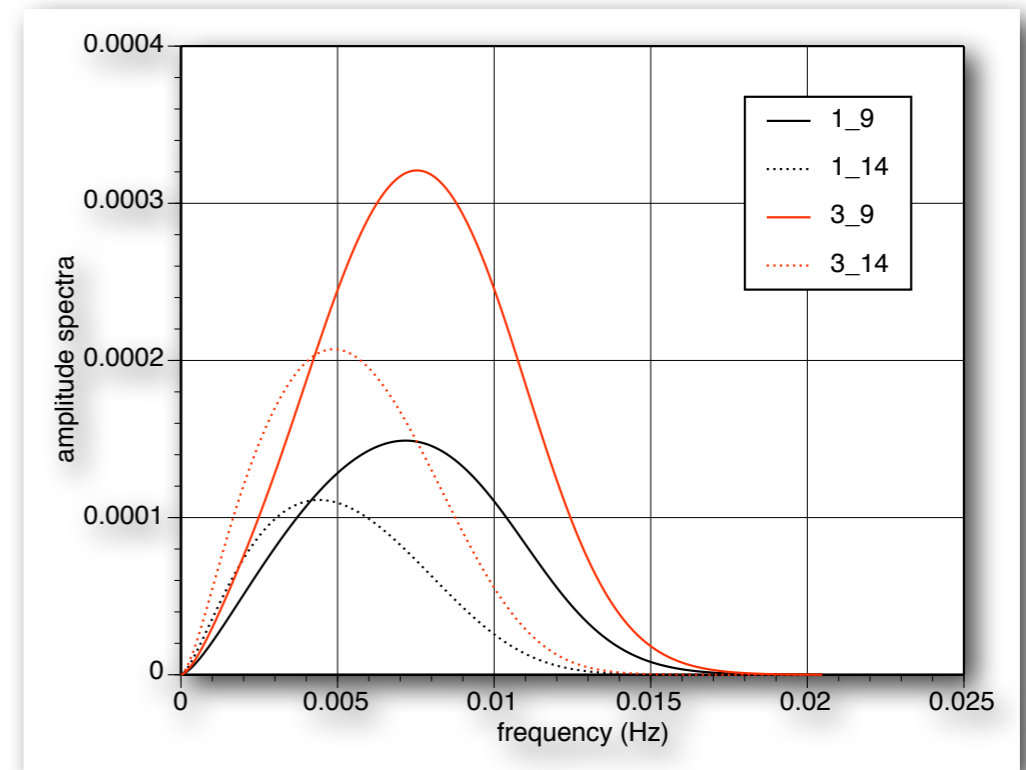
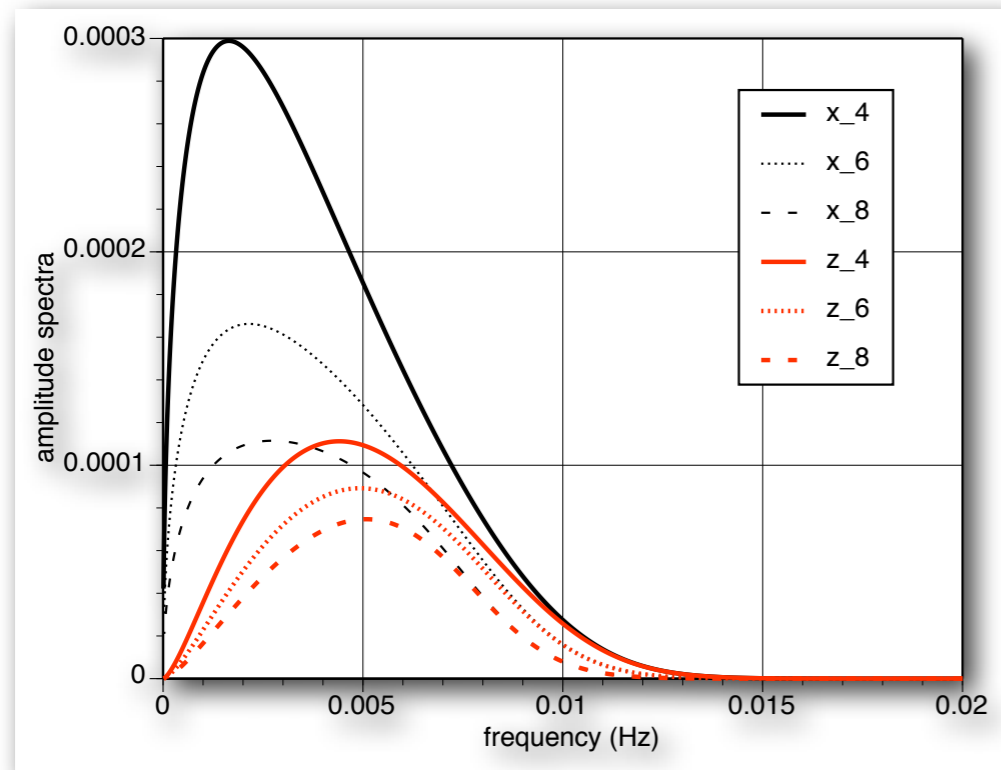
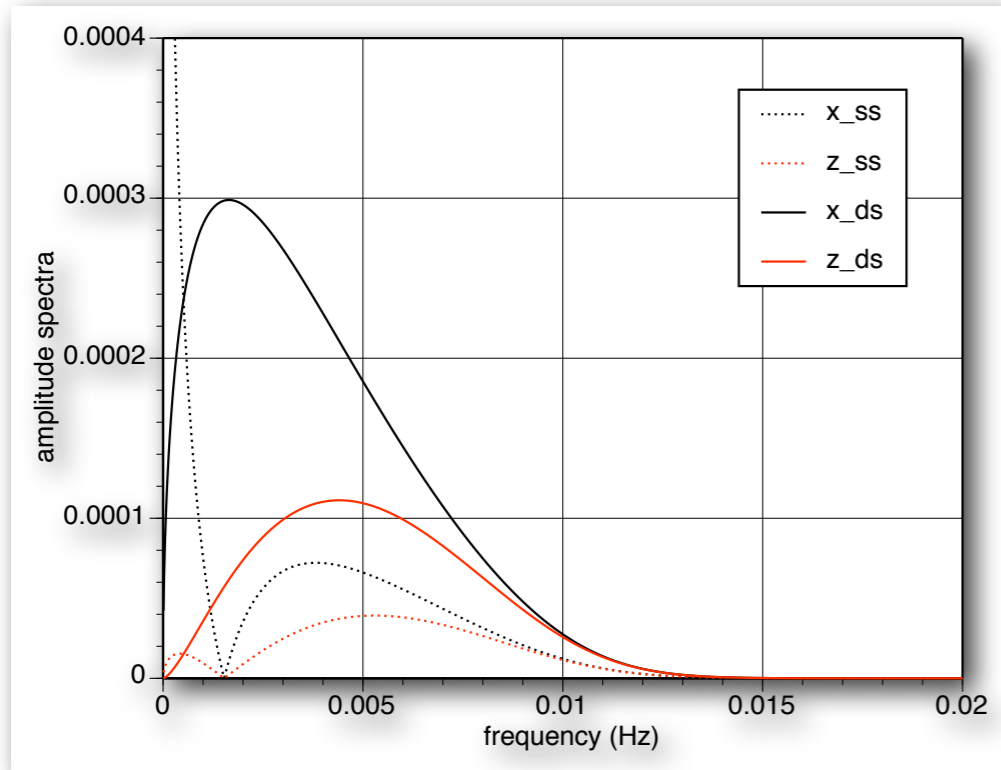
Modal approach: Eigenvalues



Eigenfunctions of the radial and vertical (normalized to 1 at the free-surface) component of motion at frequency equal to 0.007 Hz, in the fluid. The curves for three crustal models 1, 2 and 3, are totally overlapped; on the bottom, the eigenfunctions in the solid layers are shown



Modal approach: excitation spectra



Modal approach: 2D tsunami motion

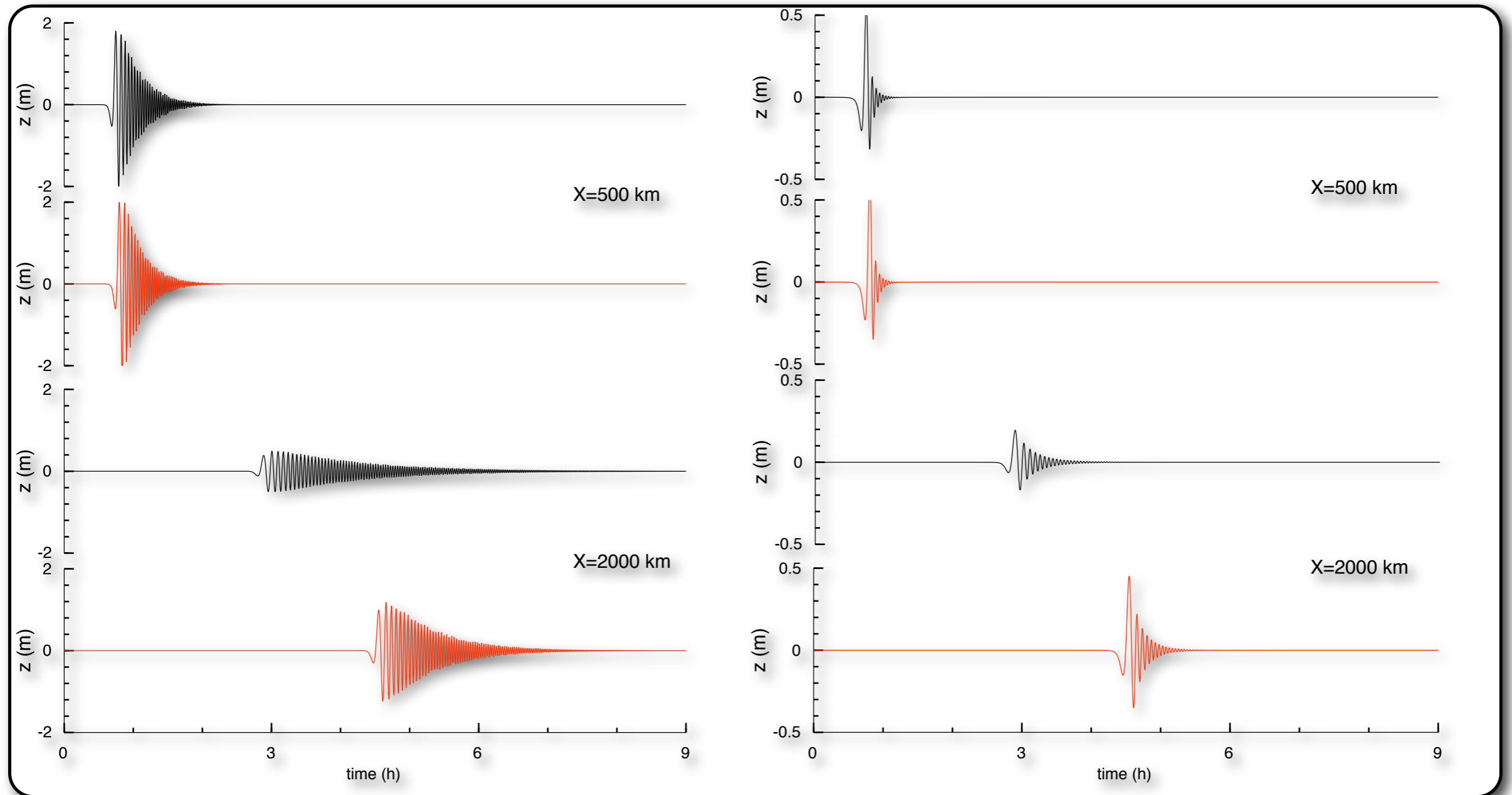
$$U(X, \varphi, z, \omega, t) = \frac{\exp(-i\pi/4)}{\sqrt{8\pi}} \frac{\exp[i\omega(t - X/c)]}{\sqrt{X}} \frac{\chi(h_s, \varphi)R(\omega)}{\sqrt{\omega c} \sqrt{v_g I_1}} \frac{\mathbf{u}(z, \omega)}{\sqrt{v_g I_1}}$$

$$U(X, \varphi, z, \omega, t) = \frac{\exp(-i\pi/4)}{\sqrt{8\pi}} \frac{\exp[i\omega(t - \tau)]}{\sqrt{J}} \frac{\chi(h_s, \varphi)R(\omega)}{\sqrt{\omega c} \sqrt{v_g I_1}} \Big|_s \frac{\mathbf{u}(z, \omega)}{\sqrt{v_g I_1}} \Big|_X$$

• SHOALING FACTOR

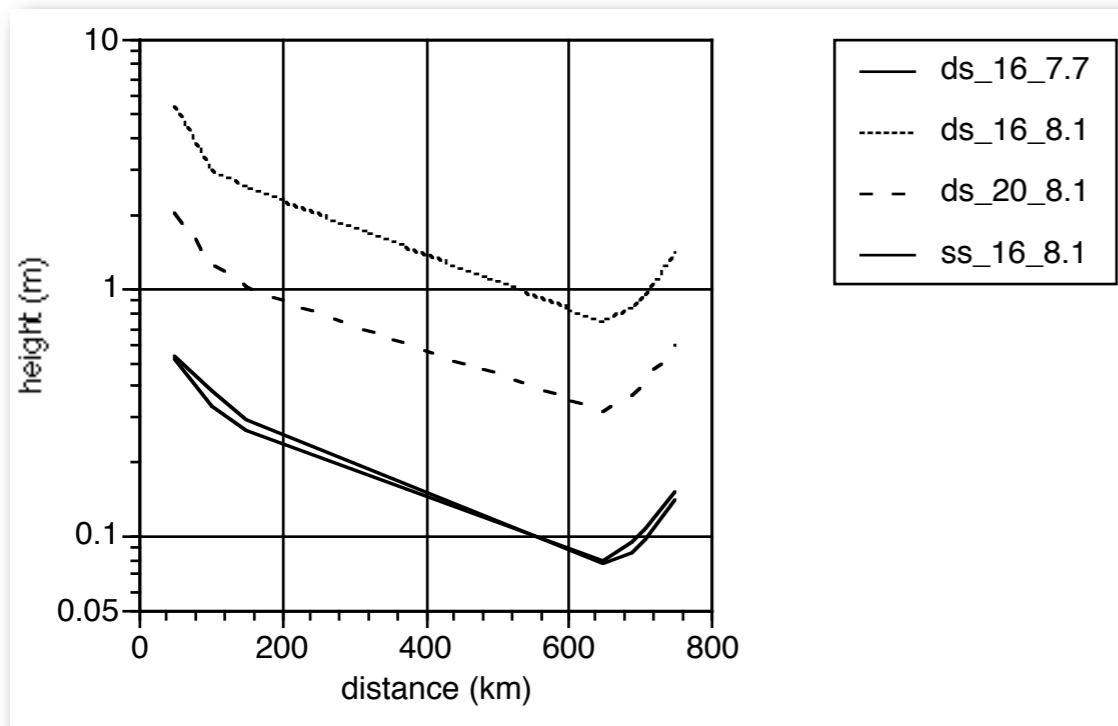
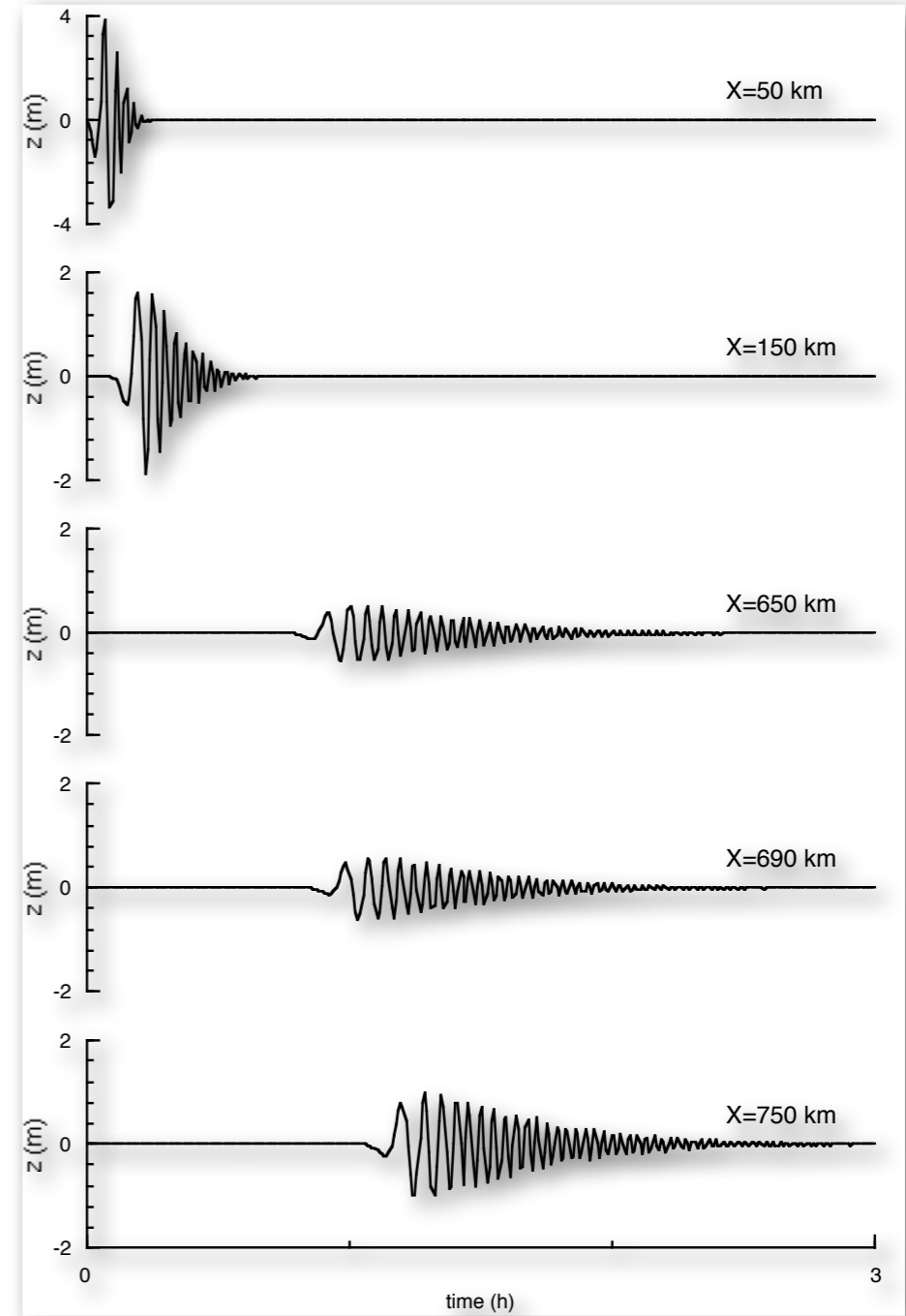
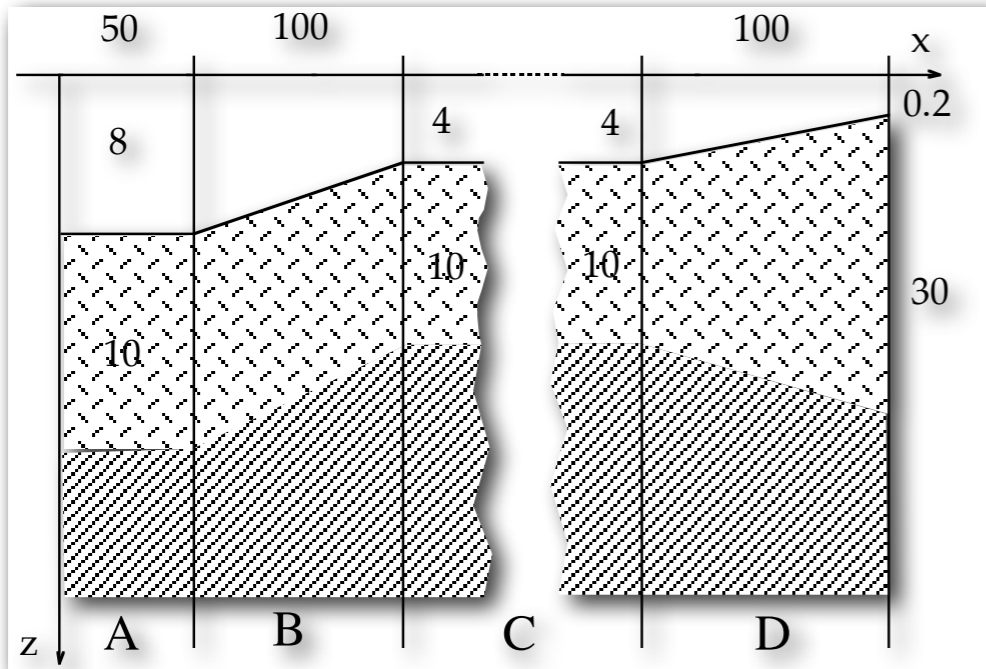
$$\left| \frac{W(X_2, 0, \omega)}{W(X_1, 0, \omega)} \right| = \left[\frac{w(0, \omega)|_2 \sqrt{v_g I_1}|_1}{w(0, \omega)|_1 \sqrt{v_g I_1}|_2} \right] \frac{\sqrt{J_1}}{\sqrt{J_2}} \cong \sqrt[4]{\frac{H_1}{H_2}}$$

Example: Synthetic signals for the tsunami mode (vertical component) excited by a dip-slip mechanism with $M_0=2.2 \cdot 10^{21}$ Nm. $h_s = 14$ km; $h_s = 34$ km.



For each of the two source-receiver distances considered, the upper trace refers to the I-D model and the lower trace to a **laterally varying model**. In the laterally varying model the liquid layer is getting thinner with increasing distance from the source, with a gradient of 0.00175 and the uppermost solid layer is compensating this thinning.

Example: Sketch of a laterally heterogeneous model for a realistic scenario. Synthetic mareograms (vertical) calculated at various distances along the section. The extension of zone C is 500 km.



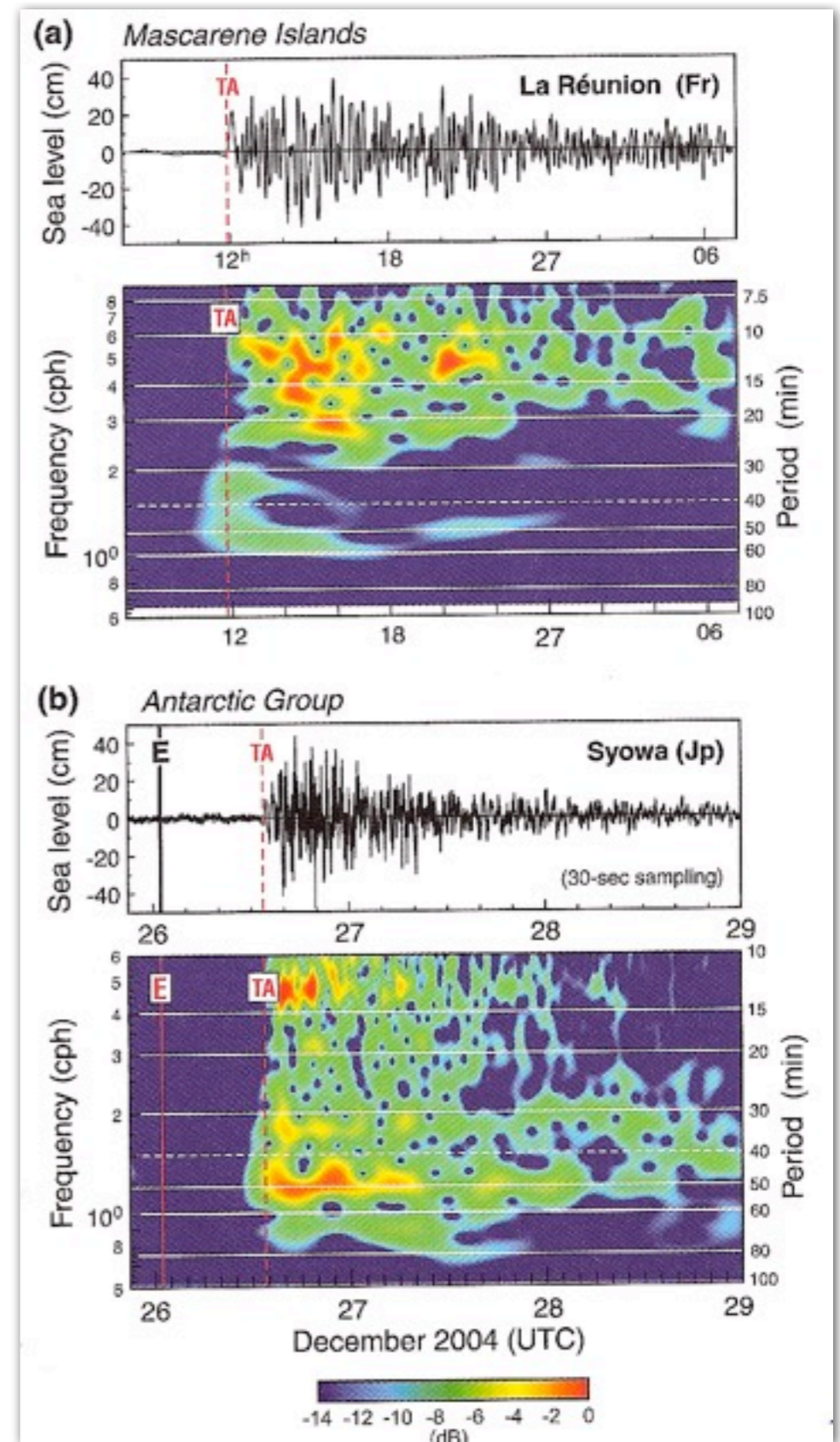
Measurement of tsunami waves

Tide gauges can measure TW along the coast...

Tsunami records and their f-t diagram: solid line (E) is the time of main shock, dashed line (TA) is Tsunami arrival

The 26 December 2004 Sumatra Tsunami: Analysis of Tide Gauge Data from the World Ocean Part I. Indian Ocean and South Africa

Alexander B. Rabinovich and Richard E. Thomson



Measurement of tsunami waves

Tide gauges can measure TW along the coast, but their detection in open ocean is challenging, due to their wavelengths and amplitudes.

ocean bottom sensors

(pressure gauges & seismometers)

Seismic Records of the 2004
Sumatra and Other Tsunamis: A
Quantitative Study

Emile A. Okal

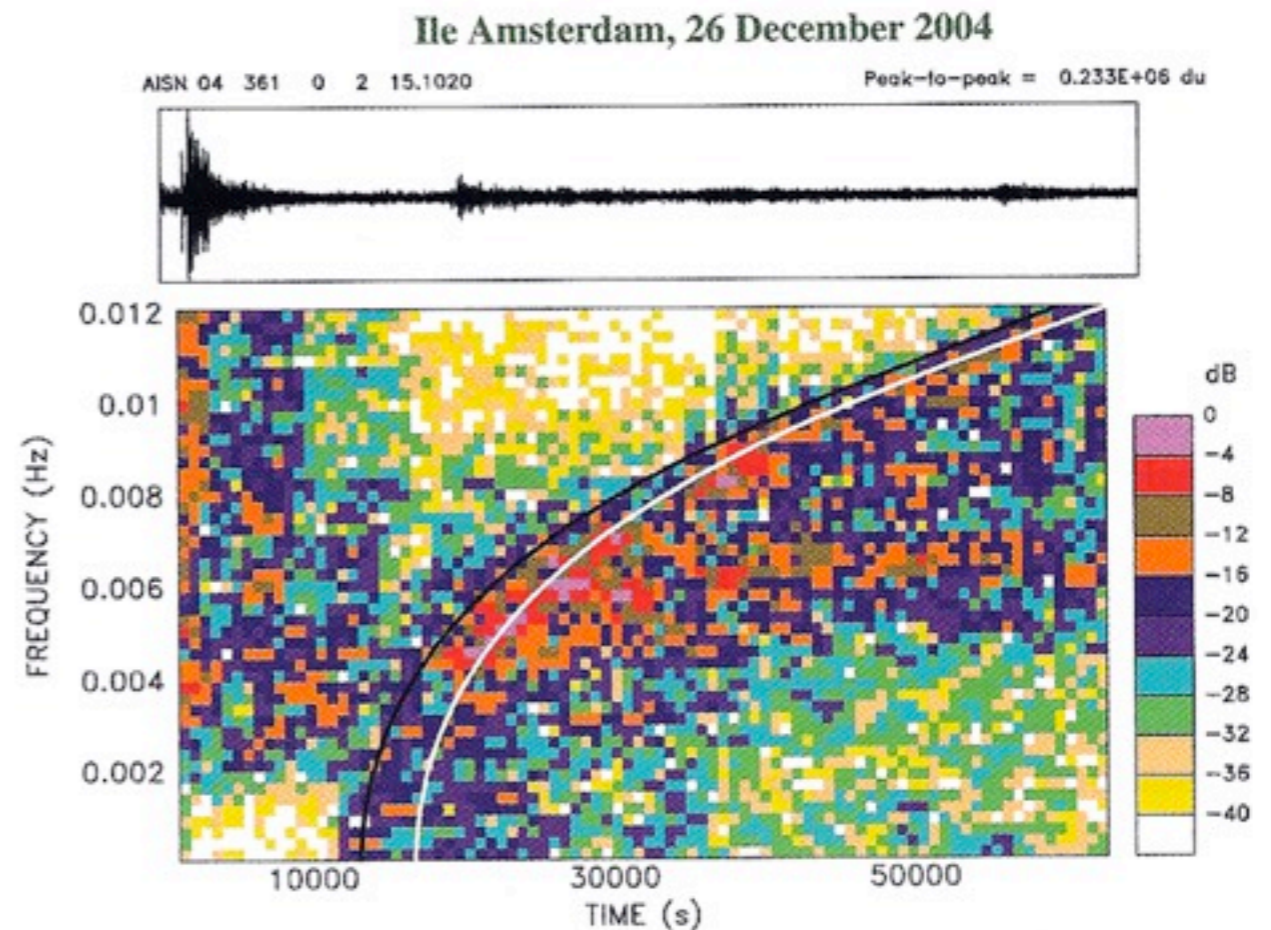


Figure 4

Spectrogram of the tsunami recording at AIS (Ile Amsterdam). The individual pixels identify the spectral amplitude present in the wave train as a function of time (abscissa) and frequency (ordinate), according to the logarithmic scale at right. In order to emphasize the high frequencies in the record, we processed the raw seismogram, without deconvolution of the instrument response. The black curve is the dispersion expected from equation (1) for a 4-km deep ocean basin and a source at the epicenter of rupture. The white curve uses a 3.5-km basin and places the source at the centroid of rupture (TSAI *et al.*, 2005).

Measurement of tsunami waves

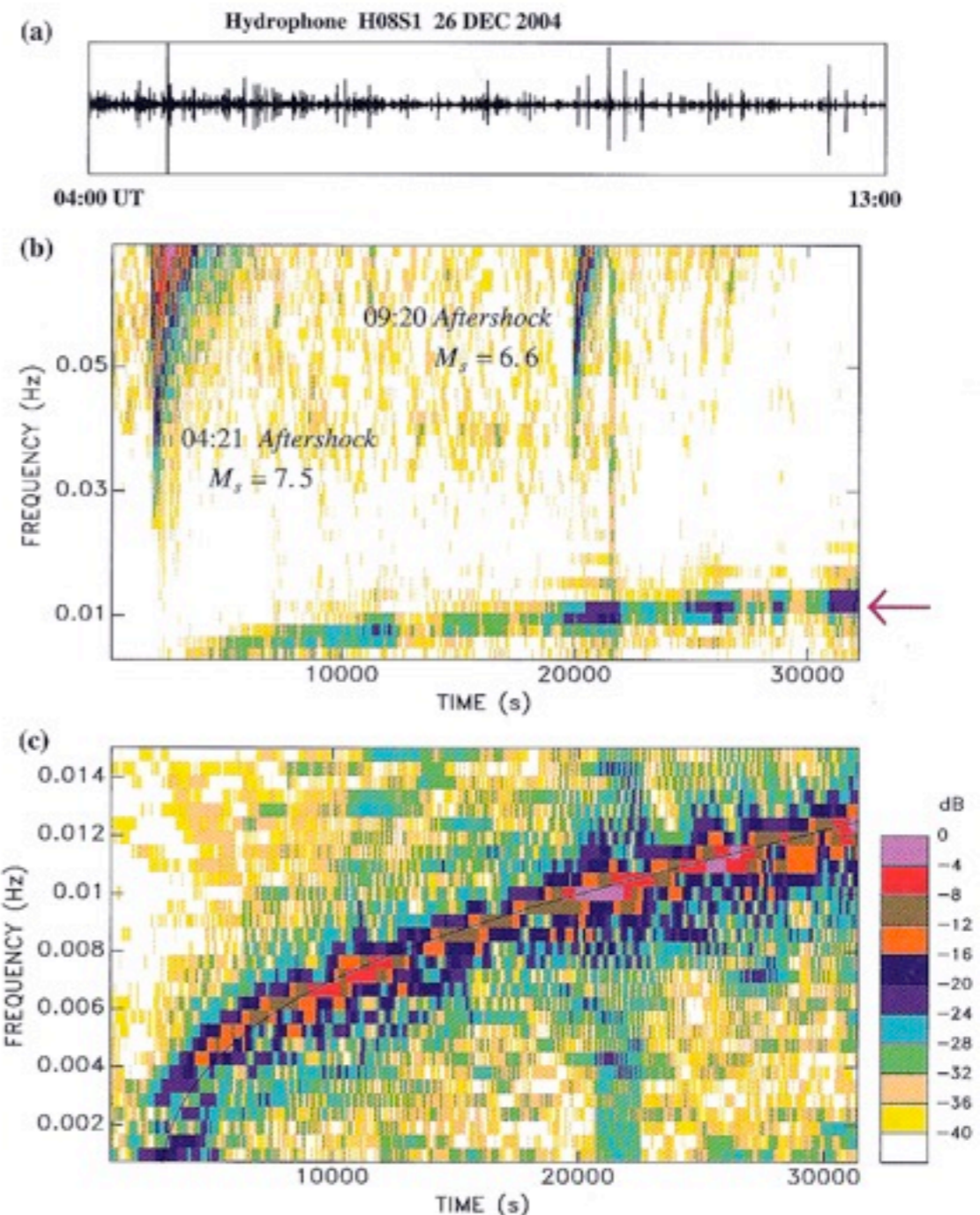
Tide gauges can measure TW along the coast, but their detection in open ocean is challenging, due to their wavelengths and amplitudes.

ocean bottom sensors

hydrophones
(towards “high” frequency bands...)

- a) Raw time series
- b) spectrogram
- c) close-up of the tsunami branch and comparison with $w^2 = gk \tanh(kH)$

Quantification of Hydrophone Records of the 2004 Sumatra Tsunami
Emile A. Okal, Jacques Talandier and Dominique Reymond



Measurement of tsunami waves

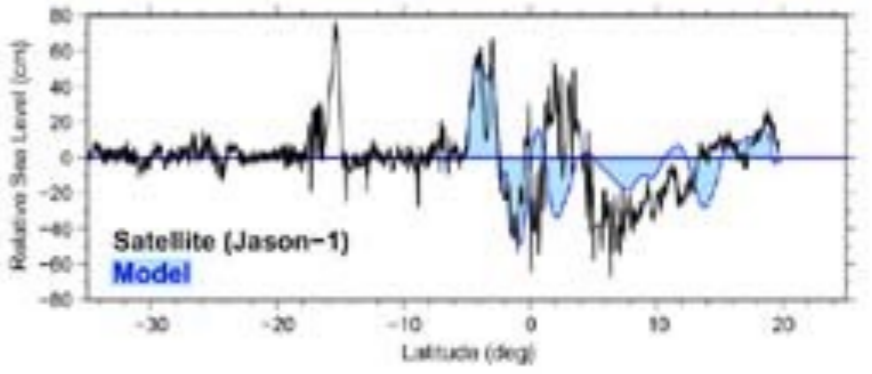
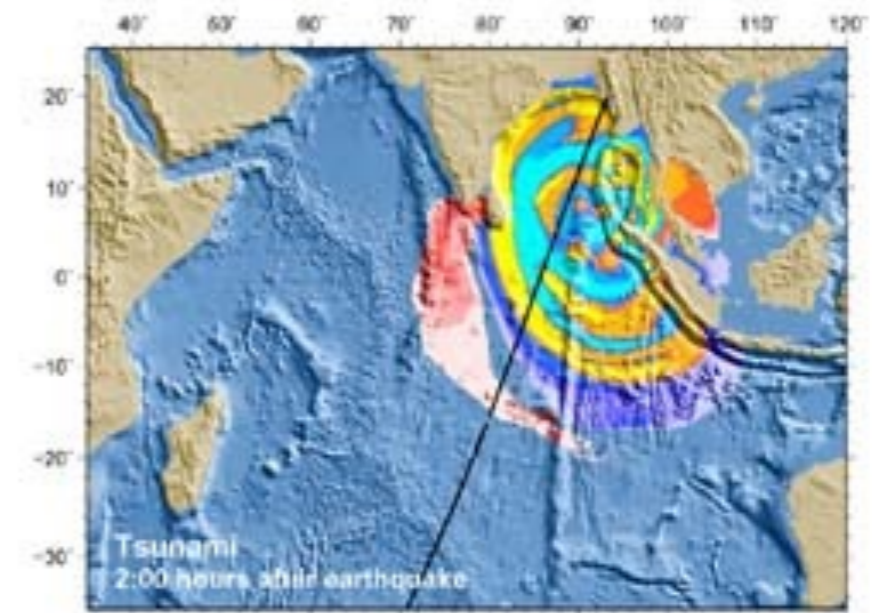
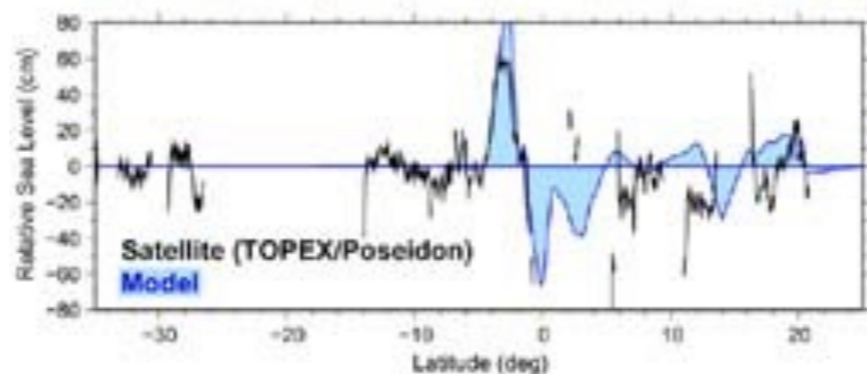
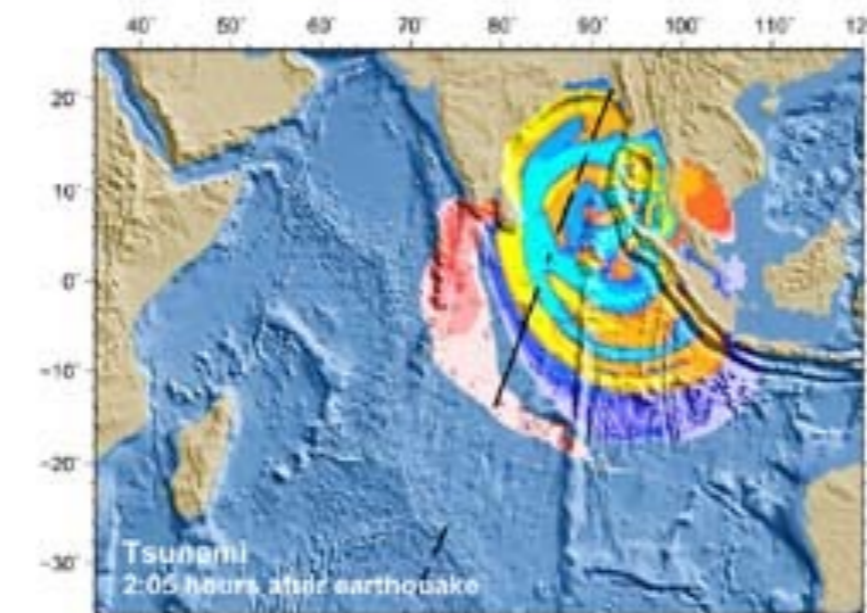
Tide gauges can measure TW along the coast, but their detection in open ocean is challenging, due to their wavelengths and amplitudes.

ocean bottom sensors (pressure gauges or seismometers)

sea level measurement (GPS receivers on buoys)

satellite altimetry

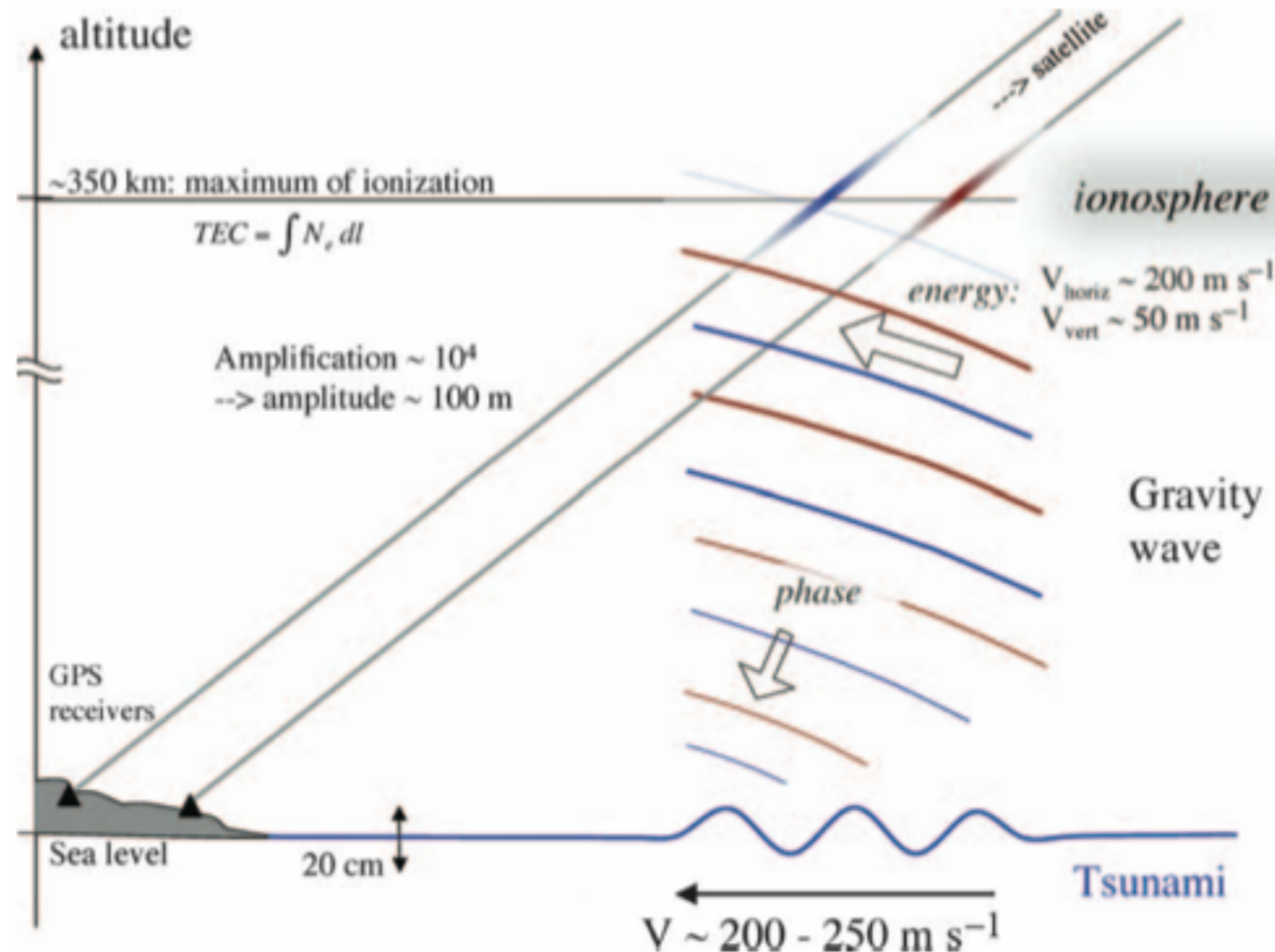
NOAA



Tsunami signature in the ionosphere

By dynamic coupling with the atmosphere, **acoustic-gravity waves** are generated

Traveling Ionospheric Disturbances (TID) can be detected and monitored by high-density GPS networks



Tsunami signature in the ionosphere

Hines (1960): atmospheric Internal Gravity Waves

Peltier & Hines (1972): can generate ionospheric signatures
in the plasma

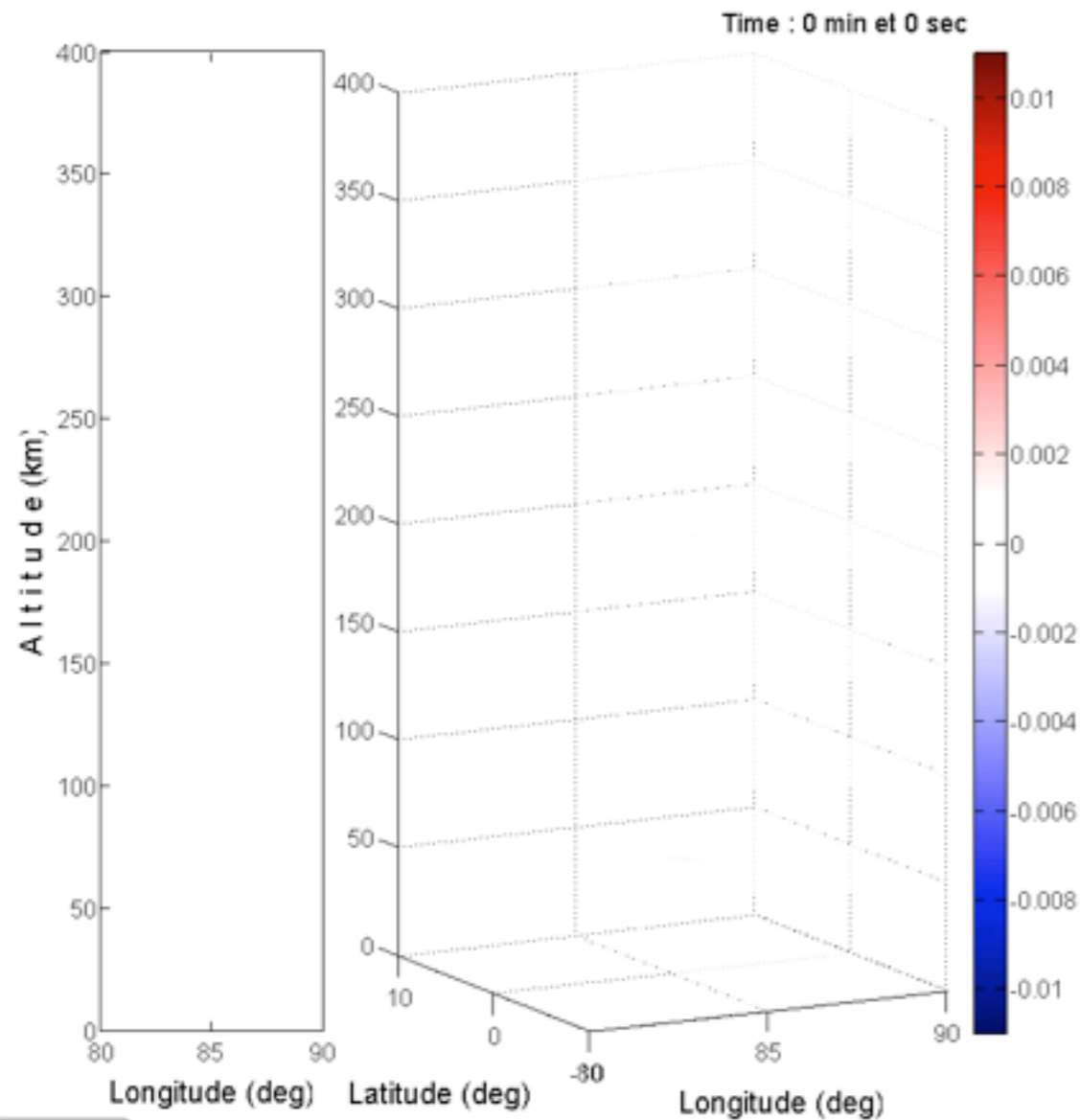
Lognonné et al. (1998): Analytical Coupled model

Artru et al. (2005): ionospheric imaging can detect tsunami
signatures. GPS JAPAN net was used to map Chilean
Tsunami of 2001

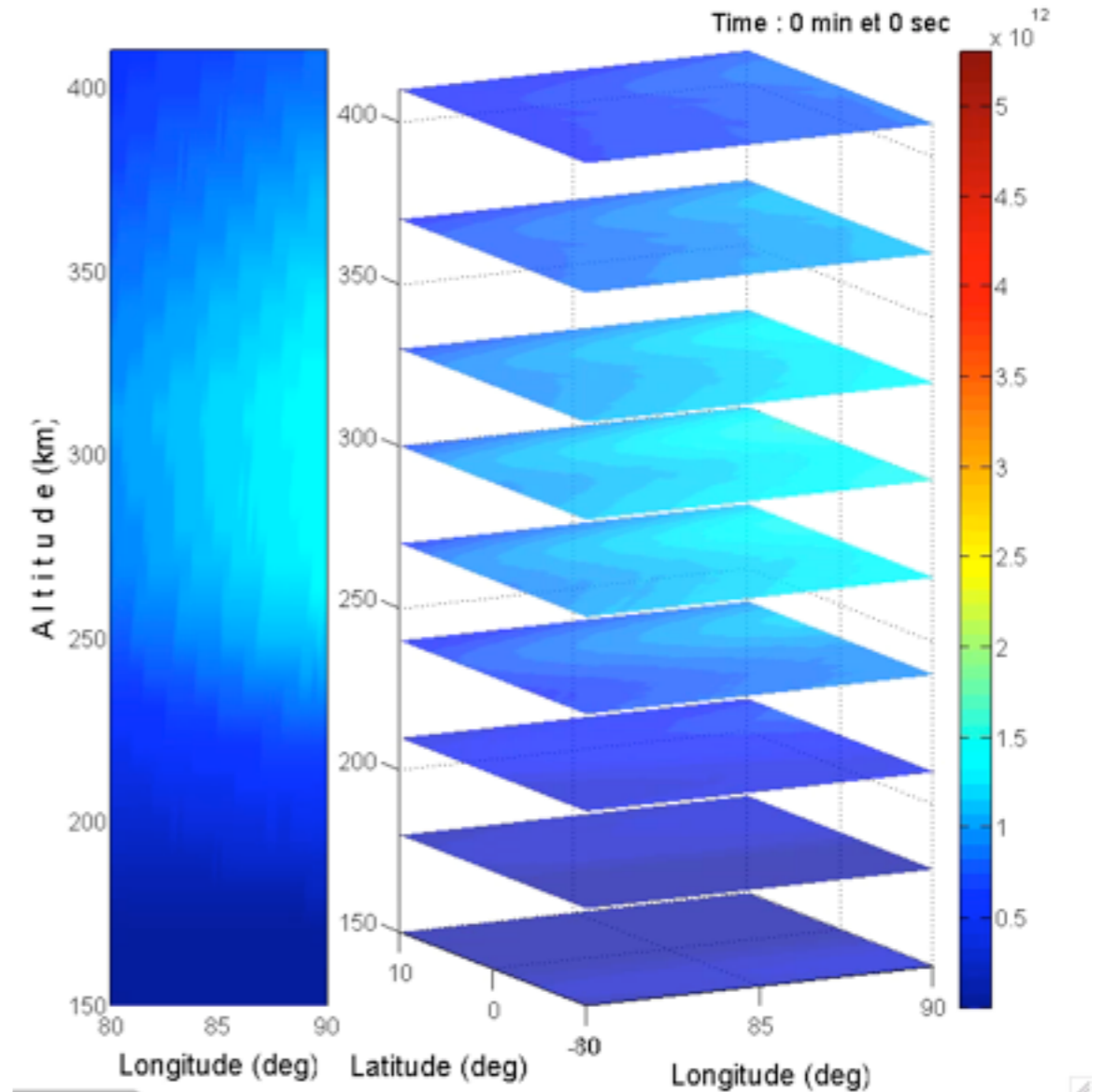
Occhipinti et al. (2006): Sumatra tsunami mapped

Tsunami signature in the ionosphere

Tsunami-generated IGWs and the response of the ionosphere to neutral motion at 2:40 UT.



Normalized vertical velocity



Perturbation in the ionospheric plasma

Tsunami signature in the ionosphere

- The TEC (Total Electron Content) perturbation induced by tsunami-coupled IGW is superimposed on a broad local-time (sunrise) TEC structure.

